

# Correlation of Attitude Effects on Slender Vehicle Transition

LARS E. ERICSSON\*

Lockheed Missiles & Space Company, Inc., Sunnyvale, California

The effects of boundary-layer transition on the motion of a slender re-entry body are large. In order to predict how transition can cause these large effects on slender vehicle stability and trim characteristics, one has to know how the vehicle attitude influences the transition geometry. Contrary to general expectations, a correlation study has shown that the percentage change from the  $\alpha = 0$  transition geometry can be defined simply as a function of the relative vehicle attitude ( $\alpha/\theta_c$ ). The windward side forward transition movement on a blunted cone is guided by entropy impingement (and associated entropy swallowing effects) in a manner that can be predicted using transition measurements at  $\alpha = 0$  in combination with embedded Newtonian theory. The leeward side forward transition movement is completely dictated by boundary layer crossflow effects and can be defined using slender cone data obtained in different ground facilities.

## Nomenclature

$d$	= body diameter
$D_N$	= nose drag, coefficient $C_{DN} = D_N/(\rho_\infty U_\infty^2/2)(\pi d_N^2/4)$
$K$	= proportionality constant, Eq. (7)
$l$	= sharp cone body length
$p$	= static pressure, coefficient $C_p = (p - p_\infty)/(\rho_\infty U_\infty^2/2)$
$r$	= body radius
$R$	= Reynolds number, $R_l = Ul/v$
$U$	= axial velocity
$x$	= axial body coordinate from sharp cone apex
$x_0$	= start of conic frustum on blunted cone
$\alpha$	= angle of attack
$\Delta$	= difference
$\theta_c$	= cone half-angle
$\nu$	= kinematic viscosity
$\rho$	= air density
$\chi$	= hypersonic similarity parameter (see Fig. 4)

## Subscripts

$AW$	= adiabatic wall
$B, N$	= base and nose, respectively
$EW$	= entropy wake impingement
$i$	= inviscid flow
$SW$	= entropy swallowing
$TR$	= transition
$W$	= wall condition
$0$	= $d_N = 0$
$\infty$	= freestream conditions

## Introduction

THE effect of boundary-layer transition on high-performance re-entry bodies has been studied by the missile industry for a long time. The early concern was with the increased aft body ablation when transition moves forward of the base,<sup>1</sup> as it could be shown experimentally<sup>2</sup> and theoretically<sup>3</sup> that the associated increased ablation rates adversely affect the vehicle damping and can lead to dynamic instability. Later it was shown both experimentally<sup>4</sup> and theoretically<sup>5</sup> that in addition to the above effect of symmetric transition, the effect of asymmetric transition on vehicle dynamics is possibly even stronger.

During recent times a great volume of experimental results has become available for the combined effects of crossflow and

nose bluntness on the transition on slender cones, both with and without mass addition.<sup>6-12</sup> In the present paper these new results are analyzed, and their importance in regard to transition effects on vehicle dynamics<sup>13</sup> is evaluated. The discussion is limited to the hypersonic and high supersonic speed ranges.

## Transition at Hypersonic Speeds

Boundary-layer transition at hypersonic speeds is a problem not yet well understood.<sup>14,15</sup> One characteristic that comes through, despite all correlation difficulties, is the rapid increase of (local) transition Reynolds number with increasing (local) Mach number—a trend that can be predicted theoretically.<sup>16</sup> Because of this trend, high-performance re-entry vehicles will have laminar flow almost down to the time of peak dynamic pressure. For this reason, transition has a dramatic effect on the vehicle aerodynamics and the re-entry vehicle motion. The effect on vehicles with ablating heatshields is particularly great owing to the overshoot of turbulent heating (and fluctuating pressure) levels.<sup>6,17</sup>

## Effect of Small Nose Bluntness on Transition

A small amount of nose bluntness produces a high entropy, low Mach number fluid layer over much of the conical frustum, which delays transition greatly.<sup>18,19</sup> The data by Softley et al.<sup>8</sup> are especially instructive in showing how boundary-layer transition depends upon the upstream swallowing of this entropy layer. When compared with the lower Mach number data of Stetson and Rushton,<sup>9</sup> however, it appears that transition occurs downstream of entropy swallowing ( $x_{SW}$ ) at  $M = 11.5$  but upstream of  $x_{SW}$  at  $M = 5.5$ . This contradiction could be the result of different definitions for completed entropy swallowing or of differences in some of the other assumptions used for the computation of  $x_{SW}$  (compare Refs. 20 and 21, for instance).

Even in the more sophisticated computations of the entropy swallowing, an effect such as the change in shear due to the dynamic pressure overshoot on a cone, described by Cleary,<sup>22</sup> is not considered. The predictions are based solely on edge unit Reynolds number and Mach number. It is clear from Morkovin's recent review of the state of the art<sup>15</sup> that we have a long way to go before we can predict transition even for a very thoroughly detailed entropy-swallowing process. It is therefore suggested here that, instead of using the somewhat ambiguous entropy-swallowing distance  $x_{SW}$  as a reference, one could use its easier-to-define inviscid counterpart, i.e., the distance  $x_{EW}$  to the completion of entropy (wake) effects on the pressure distribution. Transition will occur some distance downstream of  $x_{EW}$ ; the farther downstream the lower the freestream (unit) Reynolds

Presented as Part I of AIAA Paper 73-126 at the AIAA 11th Aerospace Sciences Meeting, Washington, D.C., January 10-12, 1973; submitted April 13, 1973; revision received November 12, 1973.

Index categories: Boundary Layer Stability and Transition; Supersonic and Hypersonic Flow.

\* Consulting Engineer. Associate Fellow AIAA.

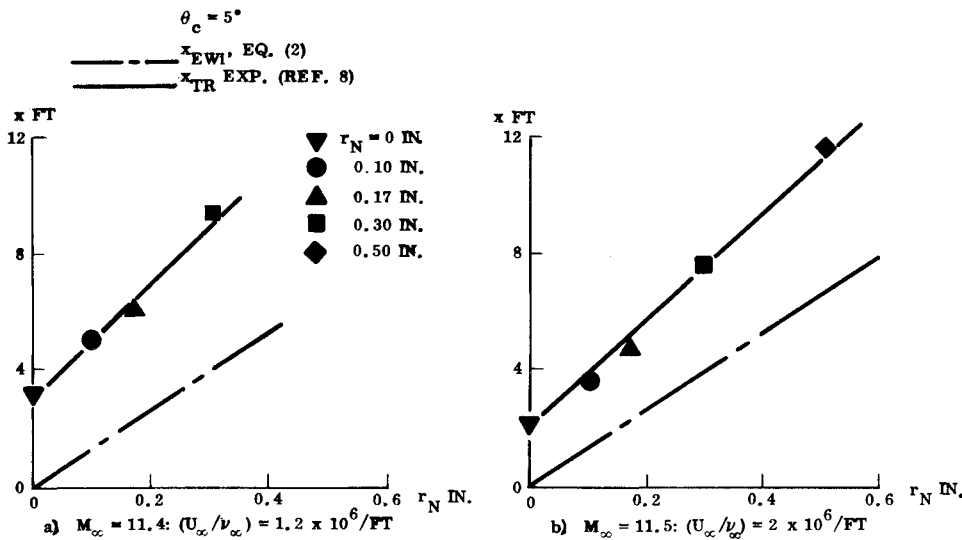


Fig. 1 Transition movement with nose bluntness.

number is (Fig. 1). One could hope that the sharp cone transition distance  $x_{TR0}$  will give a first approximation of this unit Reynolds number effect. That is

$$x_{TR} = x_{TR0} + x_{EW} + \Delta x_{TR} \quad (1)$$

Softley et al.<sup>8</sup> showed that  $R_{x_{TR}}$  was a function of  $R_{r_N}$ ; the freestream unit Reynolds number times the nose radius. The swallowing distance  $x_{SW}$  is also a function of  $R_{r_N}$ .<sup>20</sup> As  $(R_{x_{TR0}}/R_{r_N}) = x_{TR0}/r_N$ , one can expect that  $x_{TR}/x_{TR0}$  is a function  $r_N/x_{TR0}$ . The embedded Newtonian theory<sup>23</sup> gives the following definition of the inviscid value  $x_{EWi}$ :

$$x_{EWi}/r_N = (1 + 2\bar{\chi} C_{DN}^{1/2} \theta_c^{-1})/\theta_c \quad (2)$$

where  $\bar{\chi} \approx 0.6$  and  $2C_{DN}^{1/2} = 1.9$  for (hemi)spherical nose bluntness. That is,  $x_{EWi}/r_N = 163$  for the  $5^\circ$  cone used by Softley et al.<sup>8</sup> Figure 1 gives  $x_{TR}/r_N \approx 60$  for the straight line fairings† through the data for  $U_\infty/\nu_\infty = 1.2$  and  $2.0 \times 10^6/\text{ft}$ , respectively. Equation (1) can be written in the following form:

$$x_{TR}/x_{TR0} = \left[ 1 - \left( 1 + \frac{\Delta x_{TR}}{x_{EWi}} \right) \frac{x_{TR}}{x_{EWi}} \right]^{-1} \quad (3)$$

For the data in Fig. 1,  $\Delta x_{TR}/x_{EWi} = 0.37$ . Figure 2 shows that the data presented in form of  $x_{TR}/x_{TR0} = f(x_{TR}/x_{EWi})$  agree well with Eq. (3).

Martellucci's  $7.2^\circ$  cone data<sup>6,7</sup> agree also well with Eq. (3)

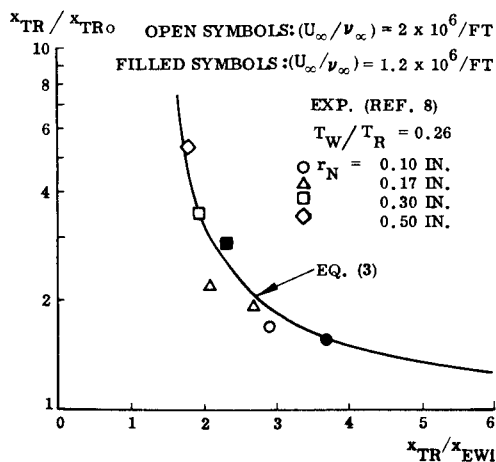


Fig. 2 Transition location relative to entropy impingement distance for a  $5^\circ$  cone at  $M_\infty \approx 11.5$ .

†The linear dependence was (first) demonstrated by the data presented by Potter and Whitfield (see Fig. 18 of Ref. 24).

( $\Delta x_{TR}/x_{EWi} = 0.70$ , see Fig. 3a). The agreement is somewhat less satisfactory for the  $8^\circ$  cone data obtained by Stetson and Rushton<sup>9</sup> [see Fig. 3b;  $\Delta x_{TR}/x_{EWi} = 0.37$ ;  $(x_{EWi})_{M=5.5}/(x_{EWi})_{M=\infty} = 0.55^\dagger$ ]. The data show a great deal of scatter, some of which is likely to be the result of getting very few data points at the same freestream unit Reynolds number. To correct shock tunnel data for unit Reynolds number effects is not a simple matter.<sup>14,26</sup>

The results shown in Figs. 2 and 3 do not imply that transition at  $\alpha = 0$  can be predicted by the use of Eqs. (2) and (3).  $\Delta x_{TR}/x_{EWi}$  is a function of both Reynolds number and Mach number. It can only be determined by experiments, where different facilities will give different values for the  $(\Delta x_{TR}/x_{EWi})$ -ratio, i.e., for the slope of the linear  $\Delta x_{TR}$  dependence<sup>8,24</sup> on  $r_N$ . What the results in Figs. 2 and 3 do mean is the following: with  $\Delta x_{TR}/x_{EWi}$  determined experimentally for  $\alpha = 0$ , Eqs. (2) and (3) will permit the  $(\alpha = 0)$ -data to be extended to  $\alpha \neq 0$ , through the use of the tangent cone approximation, to predict the nose-bluntness-induced effect on windward side transition. In this manner the great volume of data for  $\alpha = 0$  can be extended to the data-poor  $(\alpha \neq 0)$ -region. Even though the transition Reynolds number for  $\alpha = 0$  will vary greatly between test facilities, the data will give the same definition of how the normalized ("percentage") transition change varies with dimensionless attitude  $(\alpha/\theta_c)$  provided that entropy swallowing and boundary-layer crossflow effects dominate over any changes in wind-tunnel disturbance levels due to  $\alpha$ -changes. In this case the differences in  $R_{x_{TR}}$  at  $\alpha = 0$  represent simply the uncertainty in determining at what altitude transition will first occur on the re-entering slender cone.

### Effect of Angle of Attack on Transition

The large effect of angle of attack on transition was vividly demonstrated by Ward.<sup>4</sup> The leeside transition moves forward very fast with increasing angle of attack until it "freezes" at a fixed location for moderately large angles of attack. The windward side transition on the sharp cone moves back with increasing angle of attack, but the rate is almost negligible compared to the leeward side forward movement. Stetson and Rushton<sup>9</sup> showed that also the windward side transition moves forward with angle of attack if the cone is not sharp. This forward movement is, of course, a result of the movement forward of entropy wake impingement ( $x_{EWi}$ ) and associated entropy swallowing ( $x_{SW}$ ). Using the tangent cone approximation, which

<sup>†</sup>  $x_{EWi}/r_N$  is decreasing with decreasing Mach number for  $M < 10$ . Its value can be determined by the Method of Characteristics or by a less time-consuming method based on an extension of the concept of hypersonic similitude.<sup>25</sup>

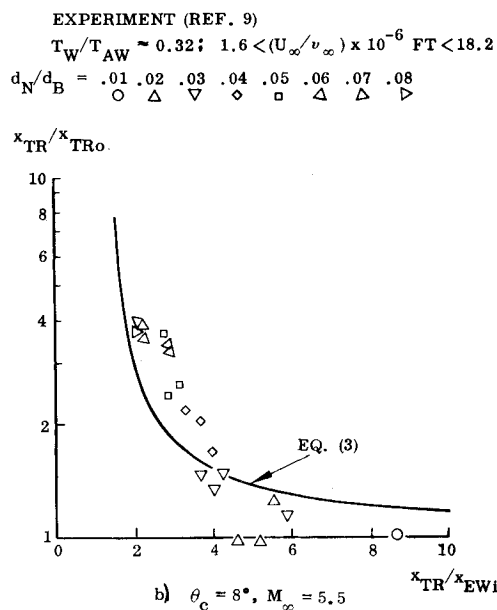
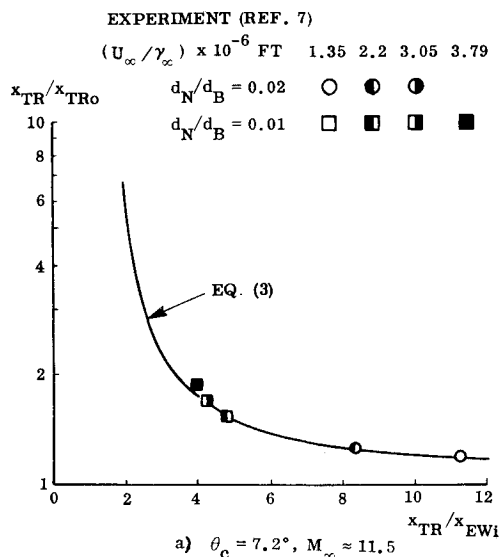


Fig. 3 Transition location relative to entropy impingement distance.

is valid for the windward side at hypersonic speeds, one can write Eq. (1) in the following form<sup>§</sup>:

$$x_{TR}(\theta_c - \alpha) = x_{TR0}(\theta_c - \alpha) + \left[ 1 + \frac{\Delta x_{TR}}{x_{EWi}} \right] x_{EWi}(\theta_c - \alpha) \quad (4)$$

where  $\Delta x_{TR}/x_{EWi}$  is assumed to remain constant. This should be a good assumption, at least for  $(\alpha/\theta_c)^2 \ll 1$ . Dropping  $\theta_c$  from the functional representation, Eq. (4) gives the following representation of the (relative) effect of angle of attack on the windward side transition:

$$\frac{x_{TR}(\alpha) - x_{TR}(0)}{x_{TR}(0)} = \frac{x_{TR0}(\alpha) - x_{TR0}(0)}{x_{TR0}(0)} \times \left[ 1 + \left( 1 + \frac{\Delta x_{TR}}{x_{EWi}} \frac{x_{EWi}(0)}{x_{TR0}(0)} \right)^{-1} + \frac{x_{EWi}(\alpha) - x_{EWi}(0)}{x_{EWi}(0)} \times \left\{ 1 + \left( 1 + \frac{\Delta x_{TR}}{x_{EWi}} \frac{x_{EWi}(0)}{x_{TR0}(0)} \right)^{-1} \right\} \right] \quad (5)$$

<sup>§</sup>  $\alpha$  is defined here as negative for the windward side, positive for the leeward side.

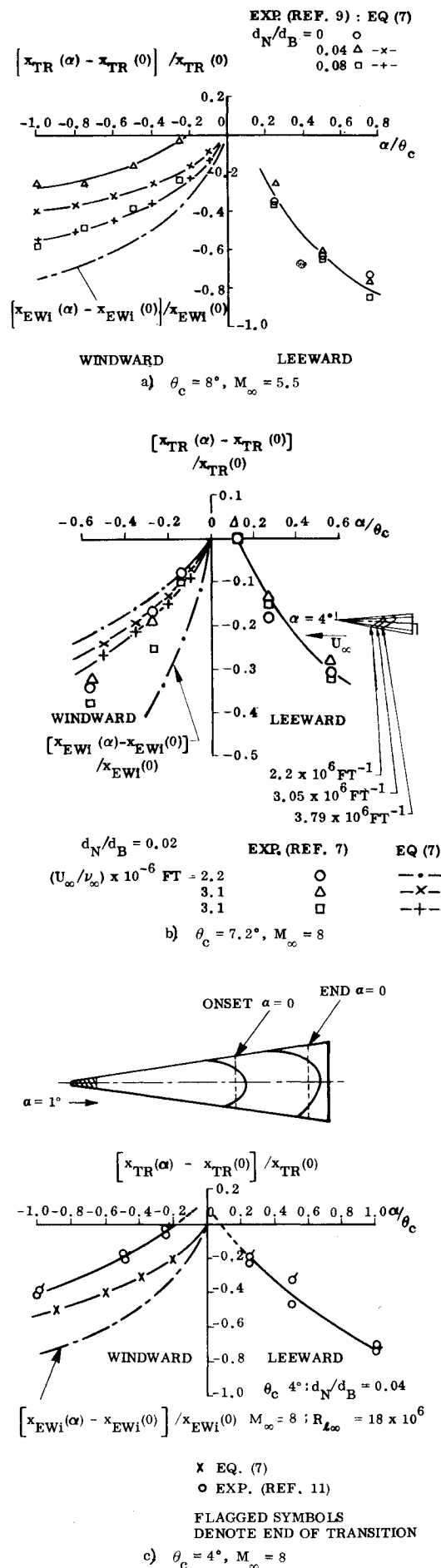


Fig. 4 Transition movement with angle of attack on slender cones.

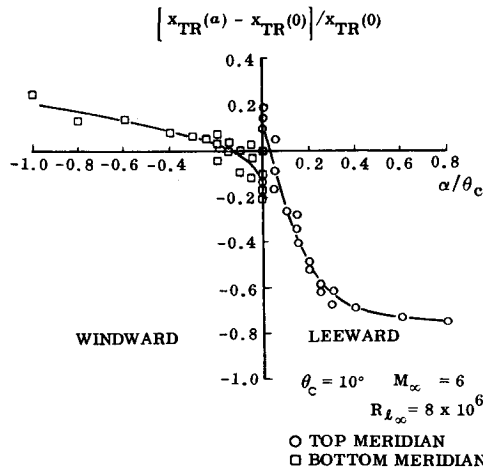


Fig. 5 Transition movement with angle of attack on 10° sharp cone at  $M_\infty = 6.4$

The sharp cone windward side aft transition movement is small compared to the forward movement due to entropy swallowing effects. It is shown in Ref. 13 that the effect of windward side transition movement on sharp cone aerodynamics is negligible for finite amplitude oscillations. Hence, one can neglect the first term on the right-hand side of Eq. (5). Substituting  $\theta_c - \alpha$  for  $\theta_c$  in Eq. (2) gives

$$\frac{x_{EWi}(\alpha)}{x_{EWi}(0)} = \frac{\left[ \left(1 - \frac{\alpha}{\theta_c}\right)^{-1} + \theta_c/2 \bar{\chi} C_{DN}^{1/2} \right] \left(1 - \frac{\alpha}{\theta_c}\right)^{-1}}{1 + \theta_c/2 \bar{\chi} C_{DN}^{1/2}} \quad (6)$$

For slender vehicles  $(\theta_c/2 \bar{\chi} C_{DN}^{1/2})^2 \ll 1$  and Eqs. (5) and (6) give

$$\frac{x_{TR}(\alpha) - x_{TR}(0)}{x_{TR}(0)} = K \left[ \left(1 - \frac{\alpha}{\theta_c}\right)^{-2} - 1 \right] \quad (7)$$

$$K = \left\{ 1 + \left[ \left(1 + \frac{\Delta x_{TR}}{x_{EWi}} \frac{x_{EWi}}{x_{TRO}} \right)^{-1} \right]^{-1} \right\}^{-1}$$

The constant  $K$  is determined by the transition data for  $\alpha = 0$  as was discussed earlier.

Figure 4 shows that Eq. (7) does a fair job in predicting the windward transition movement with dimensionless angle of attack  $\alpha/\theta_c$ . The entropy wake impingement movement, the dash-dot line in Fig. 4, is shown to indicate how close to unity  $K$  is in Eq. (7). The "zero-offset" behavior of the Stetson-Rushton data<sup>9</sup> in Fig. 4a is caused by a relatively shorter reference value  $x_{TR}(0)$  for  $d_N/d_B = 0.04$  than for  $d_N/d_B = 0.08$ . Martellucci's data<sup>8</sup> in Fig. 4b indicate an  $\alpha$ -zero-shift in addition to possible  $x_{TR}(0)$ -anomalies. This leeside movement of "true" lateral meridian is indicated by the transition front shape (see inset in Fig. 4b). The 4° cone data<sup>11\*\*</sup> in Fig. 4c indicate only the  $x_{TR}(0)$ -effect, no  $\alpha$ -zero shift (see inset). We will return to this behavior near  $\alpha = 0$  after a look at leeside transition on sharp and blunted cones.

The results shown in Fig. 4 imply that the nose-bluntness-induced entropy impingement effects dominate the windward side transition movement, and that the normalized relative transition movement  $[x_{TR}(\alpha) - x_{TR}(0)]/x_{TR}(0)$ , as a function of normalized angle of attack,  $\alpha/\theta_c$ , is predicted by Eq. (7). The proportionality constant  $K$  is determined experimentally and depends on Mach number and Reynolds number. The Mach

\* The assumption of  $K = \text{const}$  is consistent with the assumption that the tangent-cone approximation, Eq. (4), can be used.

\*\* Sharp cone transition length,  $x_{TRO}$ , was obtained by computing boundary-layer edge conditions consulting the data at the same free-stream test conditions for the 7.2° cone in Ref. 7.

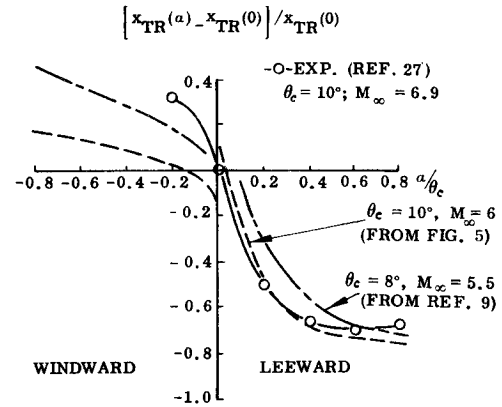


Fig. 6 Sharp cone transition movement with angle of attack at low hypersonic speeds.

number is a true parameter, whereas the Reynolds number dependence only reflects the fact that facility-induced environmental gradients determine the rate of transition advancement due to entropy impingement. Atmospheric density and temperature gradients could impose similar Reynolds number effects for the re-entering missile. However, these gradients are probably much milder than those existing in noisy ground facilities, and  $K$  in Eq. (7) will depend only upon Mach number. [Reynolds number is accounted for by use of  $x_{TR}(0)$  as a normalizing quantity.]

Ward's 10° sharp cone data<sup>4</sup> are shown in Fig. 5. The top and bottom data fairings have different intercepts at  $\alpha = 0$ . The probable reason for this will be discussed shortly. The Stetson-Rushton data<sup>9</sup> agree qualitatively with Fischer's data<sup>27</sup> for the leeside transition movement on a 10° cone at  $M = 6.9$  (see Fig. 6). At higher Mach numbers the leeside transition movement shows similar trends. Martellucci's 7.2° cone data<sup>6,7</sup> are shown in Fig. 7. DiChristina's result<sup>10</sup> for a 10° cone exhibit the same top-bottom side difference in transition characteristics for

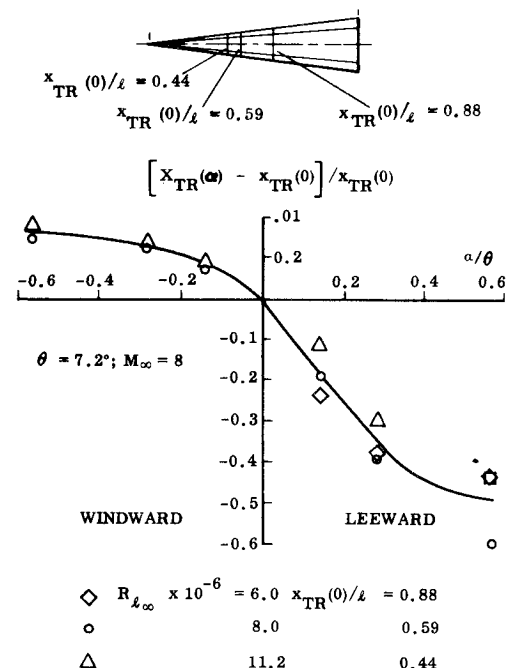


Fig. 7 Transition movement with angle of attack on a sharp 7.2° cone at  $M_\infty = 8.7$

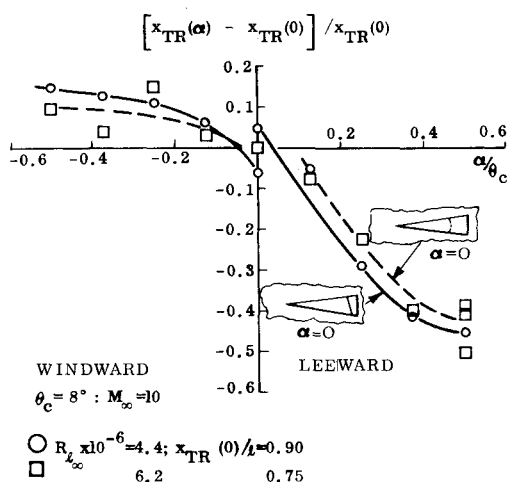


Fig. 8 Transition movement with angle of attack on an 8° sharp cone at  $M_\infty = 10.10$

$R_{L\infty} = 4.4 \times 10^6$  as Ward's data (compare Figs. 8 and 5). At  $R_{L\infty} = 6.2 \times 10^6$  the blunted-cone-type anomaly at  $\alpha = 0$  is exhibited (compare Fig. 8 and Fig. 4b). The different behaviors are explained by the transition front geometry at  $\alpha = 0$  (see insets in Figs. 4b, 5, and 8). The 10° cone data obtained by McCauley et al.<sup>28</sup> are in fair agreement with the other high Mach number data (Fig. 9).

The sharp cone transition data exhibit one outstanding characteristic, i.e., the leeside transition movement agrees reasonably well between tests in different tunnels, whereas the windward side movement shows substantial disagreement (see Figs. 6 and 9). The reason for this transition behavior is demonstrated in a very direct manner by DiChristina<sup>10</sup> (Fig. 10). On the windward side the transition Reynolds number increases as the third power of local (edge) Mach number in accordance with the general transition behavior at  $\alpha = 0$  (Ref. 16). However, on the leeward side the stabilizing†† effect of increasing local Mach number is completely overpowered by the destabilizing crossflow effects. Likewise, local flow modification due to up-

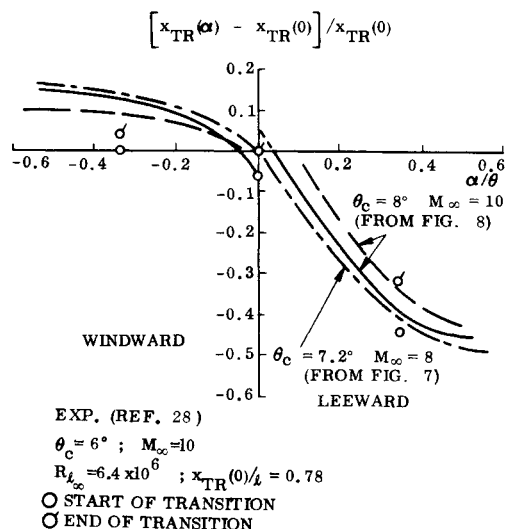


Fig. 9 Sharp cone transition movement with angle of attack at high hypersonic speeds.

†† Stabilizing = transition-delaying.

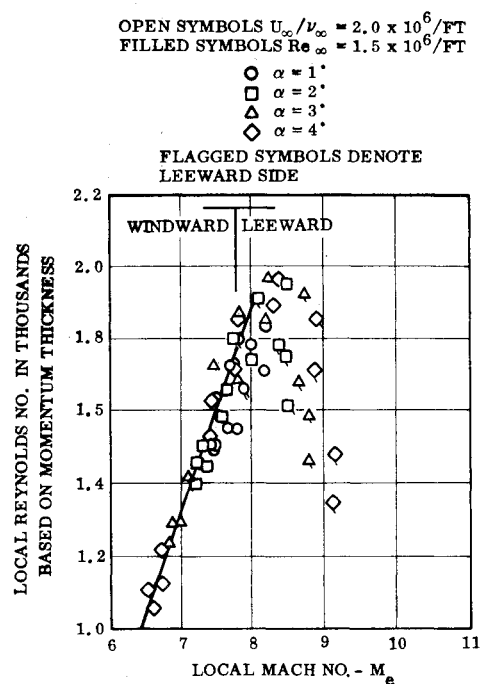


Fig. 10 Transition Reynolds number as a function of local Mach number.<sup>10</sup>

stream nose bluntness will be negligible compared to the leeside crossflow effects (see Fig. 4a).††

In Potter's review<sup>29</sup> of angle-of-attack effects on sharp cone transition, data from Refs. 30 and 31 were shown to deviate fundamentally from the other available experimental results (shown here in Figs. 5–9). The reason for the deviation of the 5° cone data of Ref. 30 is the high unit Reynolds number effect on transition Reynolds number. Depending on the selection of freestream (unit) Reynolds number, the transition movement can be forward or aft with increasing  $\alpha$  (see Fig. 14 in Ref. 30). A similar reversal of regular transition trends is exhibited by the data in Refs. 31 and 32. When unit Reynolds number was allowed to vary between windward and leeward measurements, a complete reversal of transition movement was observed<sup>33</sup> (see Fig. 2 in Ref. 31), that is, the transition moved forward on the windward side and aft on the leeward side. When the freestream (unit) Reynolds number was kept constant,<sup>31</sup> the same general reversal was observed, except for jumpwise shifts forward and aft near  $\alpha = 0$  (see Fig. 2 in Ref. 31). The high Mach number,  $M_\infty = 20$ , in combination with the slenderness,  $\theta_c = 2.87^\circ$ , undoubtedly adds complications to the regular tunnel interference problems. A windward side forward transition movement can be explained by viscous interaction effects, causing the sharp cone ( $d_N/d_B = 0.0013$ ) to appear effectively as a moderately blunt cone.<sup>33</sup> However, the windward side transition movement is dependent on local flow conditions at the edge of the boundary layer (see Fig. 10 and Refs. 34, 35). That is, the unit Reynolds number influence may overshadow the true nose bluntness effect (as was the case for  $M = 8$  in Ref. 30).

In regard to the fairing of transition data near  $\alpha = 0$ , there are basically two possibilities. Either one fair through the data getting essentially zero  $\alpha$ -slope at  $\alpha = 0$ , or one "corrects" the data for an apparent error in the reference point, i.e., the transition at  $\alpha = 0$ . The zero  $\alpha$ -slope at  $\alpha = 0$  is completely contrary to the findings by Moore<sup>36</sup> in regard to crossflow effects on laminar boundary-layer flow over sharp cones. His linear theory shows a 10° cone to have large

†† The offset anomalies for the blunted cones are discussed further later in the text.

displacement-thickness and velocity-profile  $\alpha$ -slopes at  $\alpha = 0$ , both effects contributing to forward leeside and aft windward side transition movements. On the other hand, it is well known that the transition front on a slender cone at  $\alpha = 0$  is not contained in a plane (as obviously is assumed for the data in Fig. 4c, for example). The detailed measurements performed by Nagamatsu et al.<sup>37</sup> on an 8-ft long,  $5^\circ$  sharp cone at  $M = 10$  and  $M = 14$  showed the heat-transfer rate to vary as much as  $\pm 50\%$  around the circumference at  $\alpha = 0$ . The corresponding variation of the sharp cone transition length was  $\pm 20\%$  on the forebody and  $\pm 10\%$  on the aft body. The offsets in  $\Delta x_{TR}(0)/x_{TR}(0)$  and  $\Delta\alpha/\theta_c$ , or both, in Figs. 4-9 all fall within these ranges. For a blunted cone one could speculate about other causes for the anomalous behavior at  $\alpha = 0$ , in addition to those previously discussed for the sharp cone. However, if it were a bluntness-induced flow phenomenon rather than a wind tunnel interference problem, possibly amplified by model-roughness effects, the  $8\%$  blunt cone should also have shown this behavior in Fig. 4a, not only the  $4\%$  blunt cone.

### Conclusions

Analysis of available experimental data for angle-of-attack effects on transition has produced two results of great importance for the future development of the capability to predict transition effects on slender vehicle stability and trim characteristics.

1) The windward side forward transition movement on blunted cones is guided by the entropy-wake impingement (and associated entropy swallowing effects) in a manner that is predictable from transition measurements at  $\alpha = 0$ . By the use of scaling parameters, all available slender, blunted-cone data can be used to define how this basic transition behavior depends on Mach number and unit Reynolds number. This latter parameter is a necessary evil reflecting the variation in wind tunnel disturbance level between different facilities.

2) The leeward side forward transition movement is completely dominated by boundary-layer crossflow effects. It is, for this reason, relatively insensitive to unit-Reynolds-number and nose-bluntness variations. That is, all existing experimental data can be used to define how the Mach number influences this variation of transition location with relative angle of attack,  $\alpha/\theta_c$ .

### References

- Sacks, I. and Schurmann, E. E., "Aerodynamic Phenomena Associated With Advanced Reentry Systems," AVCO-RAD-TM-63-79, Oct. 1963, Avco Corp., Greenwich, Conn., pp. 18-22.
- Grimes, J. H., Jr. and Casey, Y. Y., "Influence of Ablation on the Dynamics of Slender Re-Entry Configurations," *Journal of Spacecraft and Rockets*, Vol. 2, No. 1, Jan.-Feb. 1965, pp. 106-108.
- Ericsson, L. E. and Reding, J. P., "Ablation Effects on Vehicle Dynamics," *Journal of Spacecraft and Rockets*, Vol. 3, No. 10, Oct. 1966, pp. 1476-1483.
- Ward, L. K., "Influence of Boundary Layer Transition on Dynamic Stability at Hypersonic Speeds," Paper 6, *Transactions of the 2nd Technical Workshop on Dynamic Stability Testing*, Arnold Air Force Station, Tenn., April 20-22, 1965.
- Ericsson, L. E., "Effect of Boundary Layer Transition on Vehicle Dynamics," *Journal of Spacecraft and Rockets*, Vol. 6, No. 12, Dec. 1969, pp. 1404-1409.
- Martellucci, A. and Neff, R. S., "The Influence of Asymmetric Transition on Re-Entry Vehicle Motion," *Journal of Spacecraft and Rockets*, Vol. 8, No. 5, May 1971, pp. 476-482.
- Martellucci, A., "Asymmetric Transition Effects on the Static Stability and Motion History of a Slender Vehicle," SAMSO TR-70-141, 1970, Space and Missile Systems Organization, Air Force Systems Command, Los Angeles, Calif.
- Softley, E. J., Graber, B. C., and Zempel, R. C., "Experimental Observation of Transition of the Hypersonic Boundary Layer," *AIAA Journal*, Vol. 7, No. 2, Feb. 1969, pp. 257-263.
- Stetson, K. F. and Rushton, G. H., "A Shock Tunnel Investigation of the Effects of Nose Bluntness, Angle of Attack, and Boundary Layer Cooling on Boundary Layer Transition at a Mach Number of 5.5," *AIAA Journal*, Vol. 5, No. 5, May 1967, pp. 899-906.
- DiChristina, V., "Three-Dimensional Laminar Boundary Layer Transition on a Sharp  $8^\circ$  Cone at Mach 10," *AIAA Journal*, Vol. 8, No. 5, May 1970, pp. 852-856.
- Laganelli, A. L. and Martellucci, A., "Downstream Effects of Gaseous Injection Through a Porous Nose," AIAA Paper 72-185, San Diego, Calif., 1972.
- Martellucci, A., Chaump, L., Rogers, D., and Smith, D., "Experimental Determination of the Aero-Acoustic Environment about a Slender Cone," *AIAA Journal*, Vol. 11, No. 5, May 1973, pp. 635-642.
- Ericsson, L. E., "Transition Effects on Slender Vehicle Stability and Trim Characteristics," *Journal of Spacecraft and Rockets*, Vol. 11, No. 1, Jan. 1974, pp. 3-11.
- Morkovin, M. V., "Open Questions—Transitions to Turbulence at High Speeds, 1971," Paper 9a, Vol. III, *Proceedings of the Boundary Layer Transition Workshop*, Rept. TOR-0172 (S2816-16)-5, Nov. 3-5, 1971, The Aerospace Corp., San Bernardino, Calif.
- Morkovin, M. V., "Critical Evaluation of Transition from Laminar to Turbulent Shear Layers with Emphasis on Hypersonically Traveling Bodies," AFFDL-TR-68-149, March 1969, Air Force Flight Dynamics Lab., Wright-Patterson Air Force Base, Ohio.
- Donaldson, C. duP., Sullivan, R. D., and Yates, J. E., "An Attempt to Construct an Analytical Model of the Start of Compressible Transition," AFFDL-TR-70-153, Jan. 1971, Air Force Flight Dynamics Lab., Wright-Patterson Air Force Base, Ohio; also Paper 5, Vol. IV, *Proceedings of the Boundary Layer Transition Workshop*, Rept. TOR-0172(S2816-16)-5, Nov. 3-5, 1971, The Aerospace Corp., San Bernardino, Calif.
- Pate, S. R. and Brown, M. D., "Acoustic Measurements in Supersonic Transition Boundary Layers," AEDC TR-69-182, Oct. 1969, Arnold Engineering Development Center, Tullahoma, Tenn.
- Ferri, A. and Libby, P. A., "Note on an Interaction Between the Boundary Layer and the Inviscid Flow," *Journal of Aeronautical Sciences*, Vol. 21, No. 2, Feb. 1954, p. 130.
- Zakkay, V. and Krouse, E., "Boundary Conditions at the Outer Edge of the Boundary Layer on Blunted Conical Bodies," *AIAA Journal*, Vol. 1, No. 7, July 1963, pp. 1671, 1672.
- Zakkay, V. and Krouse, E., "Boundary Conditions at the Outer Edge of the Boundary Layer on Blunted Conical Bodies," Rept. 62-386, July 1962, Aeronautical Research Labs, Wright-Patterson Air Force Base, Dayton, Ohio.
- Moockel, W. E., "Some Effects of Bluntness on Boundary Layer Transition and Heat Transfer at Supersonic Speeds," Rept. 1312, 1957, NACA.
- Cleary, J. W., "Effects of Angle of Attack and Nose Bluntness on the Hypersonic Flow over Cones," AIAA Paper 66-414, Los Angeles, Calif., 1966.
- Ericsson, L. E., "Effect of Nose Bluntness, Angle of Attack, and Oscillation Amplitude on Hypersonic Unsteady Aerodynamics of Slender Cones," *AIAA Journal*, Vol. 9, No. 2, Feb. 1971, pp. 297-304.
- Potter, J. L. and Whitfield, J. D., "Effects of Slight Nose Bluntness and Roughness on Boundary-Layer Transition in Supersonic Flows," *Journal of Fluid Mechanics*, Vol. 12, Pt. 4, 1962, pp. 501-535.
- Chrusciel, G. T. and Hull, L. D., "Theoretical Method for Calculating Aerodynamic Characteristics of Spherically Blunted Cones," Paper 1, Vol. IV, *Transactions of the 3rd Technical Workshop on Dynamic Stability Problems*, NASA Ames Research Center, Moffet Field, Calif. Nov. 4-7, 1968.
- Morkovin, M. V., "Lessons from Transition of Shock Tube Boundary Layers," Paper 9b, Vol. III, *Proceedings of the Boundary Layer Transition Workshop*, Rept. TOR-0172-(S2816-16)-5, Nov. 3-5, 1971, The Aerospace Corp., San Bernardino, Calif.
- Fischer, M. C., "An Experimental Investigation of Boundary-Layer Transition on a  $10^\circ$  Half-Angle Cone at Mach 6.9," TND-5766, April 1970, NASA.
- McCauley, W. D., Saydah, A. R., and Bueche, J. F., "Effect of Spherical Roughness on Hypersonic Boundary-Layer Transition," *AIAA Journal*, Vol. 4, No. 12, Dec. 1966, pp. 2142-2148.
- Potter, J. L., "Some Special Features of Boundary Layer Transition on Aeroballistic Range Models," Paper 5, Vol. III, *Proceedings of the Boundary Layer Transition Workshop*, Rept. TOR-0172-(S2816-16)-5, Nov. 3-5, 1971, The Aerospace Corp., San Bernardino, Calif.
- Stainback, P. C., "Effect of Unit Reynolds Number, Nose Bluntness, Angle of Attack, and Roughness on a  $5^\circ$  Half-Angle Cone at Mach 8," TND-4961, Jan. 1969, NASA.
- Fisher, M. C. and Rudy, D. H., "Effect of Angle of Attack on

§§ At  $\alpha \neq 0$  leeside crossflow and windward side entropy-swallowing effects are dominating, and the data scatter due to a "zig-zaggy" transition front becomes relatively insignificant.

Boundary-Layer Transition at Mach 21," *AIAA Journal*, Vol. 9, No. 6, June 1971, pp. 1203-1205.

<sup>32</sup> Maddalon, D. V. and Henderson, A., Jr., "Hypersonic Transition Studies on a Slender Cone at Small Angles of Attack," *AIAA Journal*, Vol. 6, No. 1, Jan. 1968, pp. 176-177.

<sup>33</sup> Ericsson, L. E., "Universal Scaling Laws for Hypersonic Nose Bluntness Effects," *AIAA Journal*, Vol. 7, No. 12, Dec. 1969, pp. 2222-2227.

<sup>34</sup> Mateer, G. G., "Effects of Wall Cooling and Angle of Attack on Boundary-Layer Transition on Sharp Cones at  $M = 7.4$ ," Paper 4, Vol. III, *Proceeding of the Boundary Layer Transition Workshop*, Rept.

TOR-0172-(S2816-16)-5, Nov. 3-5, 1971, The Aerospace Corp., San Bernardino, Calif.

<sup>35</sup> Mateer, G. G., "The Effect of Angle of Attack on Boundary-Layer Transition on Cones," *AIAA Journal*, Vol. 10, No. 8, Aug. 1972, pp. 1127, 1128.

<sup>36</sup> Moore, F. K., "Laminar Boundary Layer on a Circular Cone in Supersonic Flow at a Small Angle of Attack," TN 2521, Oct. 1951, NACA.

<sup>37</sup> Nagamatsu, H. T., Sheer, R. E., Jr., and Graber, B. C., "Hypersonic Laminar Boundary Layer Transition on 8-Foot-Long,  $10^\circ$  Cone,  $M = 9.1-16$ ," *AIAA Journal*, Vol. 5, No. 7, July 1967, pp. 1245-1251.

APRIL 1974

AIAA JOURNAL

VOL. 12, NO. 4

# Highly Accelerated Laminar Flow at Moderately Large Reynolds Number

NOOR AFZAL\* AND V. K. LUTHRA†  
Indian Institute of Technology, Kanpur, India.

Jointly self-similar equations for first- and the second-order boundary-layer flows of an incompressible fluid with uniform freestream are studied for highly accelerated flows (Falkner-Skan pressure gradient parameter  $\beta \rightarrow \infty$ ). The first four terms in an asymptotic expansion as  $\beta \rightarrow \infty$ , for first-order and each of the second-order effects (due to longitudinal curvature, transverse curvature, and displacement) are evaluated. The results for skin friction so obtained give a good agreement with known exact results for  $\beta = 1$ . For smaller values of  $\beta$  the convergence of the series are accelerated by Eulerization, which show very good agreement with the exact results not only for  $\beta$  equal to zero but for negative values as well.

## Nomenclature

$A$	= displacement thickness due to first-order boundary layer defined by Eq. (9)
$D$	= function defined by Eq. (8)
$f$	= first-order stream function $\psi_1/\sqrt{(2\xi)}$
$F$	= second-order stream function $\psi_2/\sqrt{(2\xi)}$
$j$	= a number defined as zero for two-dimensional flow and unity for axisymmetric flow
$K$	= longitudinal surface curvature of the body
$k_t, k_r$	= longitudinal and transverse curvature parameters defined by Eqs. (6) and (7)
$n$	= coordinate normal to body
$N$	= stretched normal coordinate defined as $= R^{1/2}n$
$r$	= radius of the body
$R$	= characteristic Reynold number of the flow
$s$	= coordinate along the body
$U_1, U_2$	= first- and second-order outer flow velocities in $s$ direction
$Z$	= Eulerized variable defined as $1/(1 + \beta)$
$\xi, \eta$	= Gortler variables defined by Eq. (3)
$\alpha$	= defined as $A/(e)^{1/2}$
$\beta$	= Falkner-Skan pressure gradient parameter defined as $= 2\xi/U_1 dU_1/d\xi$

$\theta$	= angle between the axis and the tangent to the meridian curve at any point
$\varepsilon$	= $1/\beta$
$\tau_1, \tau_2$	= first- and second-order skin friction defined by Eq. (10)

## Subscripts

$\eta$	= total differentiation with respect to variable $\eta$
--------	---

## Superscripts

'	= total differentiation with respect to variable $\xi$
$d$	= displacement speed
$l$	= longitudinal curvature
$t$	= transverse curvature

## 1. Introduction

THE problem of highly accelerated flows has attracted the attention of many workers in the recent years. Under certain conditions (high acceleration, low Reynolds number effects associated with high altitude flights, etc.) laminar boundary layers are found over larger portions of the surface. Even the turbulent-boundary layers, under large pressure gradients, have been found to revert towards laminar boundary layers (Launder,<sup>1</sup> Badrinarynan and Ramjee<sup>2</sup>). Further the problem is also of interest in wind-tunnel contraction, turbine nozzle cascades, rocket nozzle, etc.

The main aim of the present work is to study the effect of large accelerations at moderately large values of Reynolds number. The oncoming stream is assumed uniform and fluid to be incompressible. Van Dyke<sup>3</sup> has proposed a theory for

Received September 7, 1973.

Index category: Boundary Layers and Convective Heat Transfer—Laminar.

\* Assistant Professor, Department of Aeronautical Engineering; present address: Department of Mechanical Engineering, Aligarh Muslim University, Aligarh, U.P.

† Graduate Student; present address: Department of Aeronautical Engineering, I.I.Sc. Bangalore.